Michel parameters and τ neutrino helicity from decay correlations in Z$\rightarrow$ $\tau^+\tau^-$

D. Buskulic, D. Casper, I. de Bonis, D. Decamp, P. Ghez, C. Goy, J.P. Lees, M.N. Minard, P. Odier, B. Pietrzyk, et al.

EUROPEAN ORGANIZATION FOR NUCLEAR RESEARCH

CERN–PPE/94–209
14 December 1994

Michel Parameters and τ Neutrino Helicity from Decay Correlations in $\mathrm{Z} \to \tau^+\tau^-$

The ALEPH Collaboration*

Abstract

The Michel parameters and the average τ–neutrino helicity are measured using correlations between the decays of the τ^+ and τ^- produced on the Z resonance and observed in the ALEPH detector at LEP . The Michel parameters, ρ_ℓ, η_ℓ, ξ_ℓ, $(\delta\xi)_\ell$, are determined from $\tau \to \ell\bar{\nu}_\ell\nu_\tau$ with $\ell = (e, \mu)$, and the average τ neutrino helicity, $\langle h(\nu_\tau)\rangle$, from $\tau \to h\nu$ with $h = (\pi, \rho, a_1)$. The results obtained with e–μ universality are: $\rho_\ell = 0.751 \pm 0.039 \pm 0.022$, $\eta_\ell = -0.04 \pm 0.15 \pm 0.11$, $\xi_\ell = 1.18 \pm 0.15 \pm 0.06$, $(\delta\xi)_\ell = 0.88 \pm 0.11 \pm 0.07$, and the average τ neutrino helicity $\langle h(\nu_\tau)\rangle = -1.006 \pm 0.032 \pm 0.019$. No significant deviation from the Standard Model V-A prediction is observed.

(to be submitted to Physics Letters B)

*See the following pages for the list of authors.

The ALEPH Collaboration

D. Buskulic, D. Casper, I. De Bonis, D. Decamp, P. Ghez, C. Goy, J.-P. Lees, M.-N. Minard, P. Odier, B. Pietrzyk

Laboratoire de Physique des Particules (LAPP), IN^2P^3-CNRS, 74019 Annecy-le-Vieux Cedex, France

F. Ariztizabal, M. Chmeissani, J.M. Crespo, I. Efthymiopoulos, E. Fernandez, M. Fernandez-Bosman, V. Gaitan, Ll. Garrido,[15] M. Martinez, S. Orteu, A. Pacheco, C. Padilla, F. Palla, A. Pascual, J.A. Perlas, F. Sanchez, F. Teubert

Institut de Fisica d'Altes Energies, Universitat Autonoma de Barcelona, 08193 Bellaterra (Barcelona), Spain[7]

D. Creanza, M. de Palma, A. Farilla, G. Iaselli, G. Maggi,[3] N. Marinelli, S. Natali, S. Nuzzo, A. Ranieri, G. Raso, F. Romano, F. Ruggieri, G. Selvaggi, L. Silvestris, P. Tempesta, G. Zito

Dipartimento di Fisica, INFN Sezione di Bari, 70126 Bari, Italy

X. Huang, J. Lin, Q. Ouyang, T. Wang, Y. Xie, R. Xu, S. Xue, J. Zhang, L. Zhang, W. Zhao

Institute of High-Energy Physics, Academia Sinica, Beijing, The People's Republic of China[8]

G. Bonvicini, M. Cattaneo, P. Comas, P. Coyle, H. Drevermann, A. Engelhardt, R.W. Forty, M. Frank, G. Ganis, M. Girone, R. Hagelberg, J. Harvey, R. Jacobsen,[24] B. Jost, J. Knobloch, I. Lehraus, M. Maggi, C. Markou,[27] E.B. Martin, P. Mato, H. Meinhard, A. Minten, R. Miquel, P. Palazzi, J.R. Pater, P. Perrodo, J.-F. Pusztaszeri, F. Ranjard, L. Rolandi, D. Schlatter, M. Schmelling, W. Tejessy, I.R. Tomalin, R. Veenhof, A. Venturi, H. Wachsmuth, W. Wiedenmann, T. Wildish, W. Witzeling, J. Wotschack

European Laboratory for Particle Physics (CERN), 1211 Geneva 23, Switzerland

Z. Ajaltouni, M. Bardadin-Otwinowska,[2] A. Barres, C. Boyer, A. Falvard, P. Gay, C. Guicheney, P. Henrard, J. Jousset, B. Michel, S. Monteil, J-C. Montret, D. Pallin, P. Perret, F. Podlyski, J. Proriol, J.-M. Rossignol, F. Saadi

Laboratoire de Physique Corpusculaire, Université Blaise Pascal, IN^2P^3-CNRS, Clermont-Ferrand, 63177 Aubière, France

T. Fearnley, J.B. Hansen, J.D. Hansen, J.R. Hansen, P.H. Hansen, S.D. Johnson, B.S. Nilsson

Niels Bohr Institute, 2100 Copenhagen, Denmark[9]

A. Kyriakis, E. Simopoulou, I. Siotis, A. Vayaki, K. Zachariadou

Nuclear Research Center Demokritos (NRCD), Athens, Greece

A. Blondel, G. Bonneaud, J.C. Brient, P. Bourdon, L. Passalacqua, A. Rougé, M. Rumpf, R. Tanaka, A. Valassi, M. Verderi, H. Videau

Laboratoire de Physique Nucléaire et des Hautes Energies, Ecole Polytechnique, IN^2P^3-CNRS, 91128 Palaiseau Cedex, France

D.J. Candlin, M.I. Parsons, E. Veitch

Department of Physics, University of Edinburgh, Edinburgh EH9 3JZ, United Kingdom[10]

E. Focardi, G. Parrini

Dipartimento di Fisica, Università di Firenze, INFN Sezione di Firenze, 50125 Firenze, Italy

M. Corden, M. Delfino,[12] C. Georgiopoulos, D.E. Jaffe

Supercomputer Computations Research Institute, Florida State University, Tallahassee, FL 32306-4052, USA [13,14]

A. Antonelli, G. Bencivenni, G. Bologna,[4] F. Bossi, P. Campana, G. Capon, F. Cerutti, V. Chiarella, G. Felici, P. Laurelli, G. Mannocchi,[5] F. Murtas, G.P. Murtas, M. Pepe-Altarelli, S. Salomone

Laboratori Nazionali dell'INFN (LNF-INFN), 00044 Frascati, Italy

P. Colrain, I. ten Have,[6] I.G. Knowles, J.G. Lynch, W. Maitland, W.T. Morton, C. Raine, P. Reeves, J.M. Scarr, K. Smith, M.G. Smith, A.S. Thompson, S. Thorn, R.M. Turnbull

Department of Physics and Astronomy, University of Glasgow, Glasgow G12 8QQ,United Kingdom[10]

U. Becker, O. Braun, C. Geweniger, G. Graefe, P. Hanke, V. Hepp, E.E. Kluge, A. Putzer, B. Rensch, M. Schmidt, J. Sommer, H. Stenzel, K. Tittel, M. Wunsch

Institut für Hochenergiephysik, Universität Heidelberg, 69120 Heidelberg, Fed. Rep. of Germany[16]

R. Beuselinck, D.M. Binnie, W. Cameron, D.J. Colling, P.J. Dornan, N. Konstantinidis, L. Moneta, A. Moutoussi, J. Nash, G. San Martin, J.K. Sedgbeer, A.M. Stacey

Department of Physics, Imperial College, London SW7 2BZ, United Kingdom[10]

G. Dissertori, P. Girtler, E. Kneringer, D. Kuhn, G. Rudolph

Institut für Experimentalphysik, Universität Innsbruck, 6020 Innsbruck, Austria[18]

C.K. Bowdery, T.J. Brodbeck, A.J. Finch, F. Foster, G. Hughes, D. Jackson, N.R. Keemer, M. Nuttall, A. Patel, T. Sloan, S.W. Snow, E.P. Whelan

Department of Physics, University of Lancaster, Lancaster LA1 4YB, United Kingdom[10]

A. Galla, A.M. Greene, K. Kleinknecht, J. Raab, B. Renk, H.-G. Sander, H. Schmidt, S.M. Walther, R. Wanke, B. Wolf

Institut für Physik, Universität Mainz, 55099 Mainz, Fed. Rep. of Germany[16]

J.J. Aubert, A.M. Bencheikh, C. Benchouk, A. Bonissent, G. Bujosa, D. Calvet, J. Carr, C. Diaconu, F. Etienne, M. Thulasidas, D. Nicod, P. Payre, D. Rousseau, M. Talby

Centre de Physique des Particules, Faculté des Sciences de Luminy, IN^{2}P^3-CNRS, 13288 Marseille, France

I. Abt, R. Assmann, C. Bauer, W. Blum, D. Brown,[24] H. Dietl, F. Dydak,[21] C. Gotzhein, A.W. Halley, K. Jakobs, H. Kroha, G. Lütjens, G. Lutz, W. Männer, H.-G. Moser, R. Richter, A. Rosado-Schlosser, A.S. Schwarz,[23] R. Settles, H. Seywerd, U. Stierlin,[2] R. St. Denis, G. Wolf

Max-Planck-Institut für Physik, Werner-Heisenberg-Institut, 80805 München, Fed. Rep. of Germany[16]

R. Alemany, J. Boucrot, O. Callot, A. Cordier, F. Courault, M. Davier, L. Duflot, J.-F. Grivaz, Ph. Heusse, M. Jacquet, P. Janot, D.W. Kim,[19] F. Le Diberder, J. Lefrançois, A.-M. Lutz, G. Musolino, I. Nikolic, H.J. Park, I.C. Park, M.-H. Schune, S. Simion, J.-J. Veillet, I. Videau

Laboratoire de l'Accélérateur Linéaire, Université de Paris-Sud, IN^{2}P^3-CNRS, 91405 Orsay Cedex, France

D. Abbaneo, G. Bagliesi, G. Batignani, S. Bettarini, U. Bottigli, C. Bozzi, G. Calderini, M. Carpinelli, M.A. Ciocci, V. Ciulli, R. Dell'Orso, I. Ferrante, F. Fidecaro, L. Foà,[1] F. Forti, A. Giassi, M.A. Giorgi, A. Gregorio, F. Ligabue, A. Lusiani, P.S. Marrocchesi, A. Messineo, G. Rizzo, G. Sanguinetti, A. Sciabà, P. Spagnolo, J. Steinberger, R. Tenchini, G. Tonelli,[26] G. Triggiani, C. Vannini, P.G. Verdini, J. Walsh

Dipartimento di Fisica dell'Università, INFN Sezione di Pisa, e Scuola Normale Superiore, 56010 Pisa, Italy

A.P. Betteridge, G.A. Blair, L.M. Bryant, Y. Gao, M.G. Green, D.L. Johnson, T. Medcalf, Ll.M. Mir, J.A. Strong

Department of Physics, Royal Holloway & Bedford New College, University of London, Surrey TW20 OEX, United Kingdom[10]

V. Bertin, D.R. Botterill, R.W. Clifft, T.R. Edgecock, S. Haywood, M. Edwards, P. Maley, P.R. Norton, J.C. Thompson

Particle Physics Dept., Rutherford Appleton Laboratory, Chilton, Didcot, Oxon OX11 OQX, United Kingdom[10]

B. Bloch-Devaux, P. Colas, H. Duarte, S. Emery, W. Kozanecki, E. Lançon, M.C. Lemaire, E. Locci, B. Marx, P. Perez, J. Rander, J.-F. Renardy, A. Rosowsky, A. Roussarie, J.-P. Schuller, J. Schwindling, D. Si Mohand, A. Trabelsi, B. Vallage

CEA, DAPNIA/Service de Physique des Particules, CE-Saclay, 91191 Gif-sur-Yvette Cedex, France[17]

R.P. Johnson, A.M. Litke, G. Taylor, J. Wear

Institute for Particle Physics, University of California at Santa Cruz, Santa Cruz, CA 95064, USA[22]

A. Beddall, C.N. Booth, R. Boswell, S. Cartwright, F. Combley, I. Dawson, A. Koksal, M. Letho, W.M. Newton, C. Rankin, L.F. Thompson

Department of Physics, University of Sheffield, Sheffield S3 7RH, United Kingdom[10]

A. Böhrer, S. Brandt, G. Cowan, E. Feigl, C. Grupen, G. Lutters, J. Minguet-Rodriguez, F. Rivera,[25] P. Saraiva, U. Schäfer, L. Smolik

Fachbereich Physik, Universität Siegen, 57068 Siegen, Fed. Rep. of Germany[16]

L. Bosisio, R. Della Marina, G. Giannini, B. Gobbo, L. Pitis, F. Ragusa[20]

Dipartimento di Fisica, Università di Trieste e INFN Sezione di Trieste, 34127 Trieste, Italy

H. Kim, J. Rothberg, S. Wasserbaech

Experimental Elementary Particle Physics, University of Washington, WA 98195 Seattle, U.S.A.

S.R. Armstrong, L. Bellantoni, P. Elmer, Z. Feng, D.P.S. Ferguson, Y.S. Gao, S. González, J. Grahl, J.L. Harton, O.J. Hayes, H. Hu, P.A. McNamara III, J.M. Nachtman, W. Orejudos, Y.B. Pan, Y. Saadi, M. Schmitt, I.J. Scott, V. Sharma, J.D. Turk, A.M. Walsh, F.V. Weber,[1] Sau Lan Wu, X. Wu, J.M. Yamartino, M. Zheng, G. Zobernig

Department of Physics, University of Wisconsin, Madison, WI 53706, USA[11]

[1]Now at CERN, 1211 Geneva 23, Switzerland.
[2]Deceased.
[3]Now at Dipartimento di Fisica, Università di Lecce, 73100 Lecce, Italy.
[4]Also Istituto di Fisica Generale, Università di Torino, Torino, Italy.
[5]Also Istituto di Cosmo-Geofisica del C.N.R., Torino, Italy.
[6]Now at TSM Business School, Enschede, The Netherlands.
[7]Supported by CICYT, Spain.
[8]Supported by the National Science Foundation of China.
[9]Supported by the Danish Natural Science Research Council.
[10]Supported by the UK Science and Engineering Research Council.
[11]Supported by the US Department of Energy, contract DE-AC02-76ER00881.
[12]On leave from Universitat Autonoma de Barcelona, Barcelona, Spain.
[13]Supported by the US Department of Energy, contract DE-FG05-92ER40742.
[14]Supported by the US Department of Energy, contract DE-FC05-85ER250000.
[15]Permanent address: Universitat de Barcelona, 08208 Barcelona, Spain.
[16]Supported by the Bundesministerium für Forschung und Technologie, Fed. Rep. of Germany.
[17]Supported by the Direction des Sciences de la Matière, C.E.A.
[18]Supported by Fonds zur Förderung der wissenschaftlichen Forschung, Austria.
[19]Permanent address: Kangnung National University, Kangnung, Korea.
[20]Now at Dipartimento di Fisica, Università di Milano, Milano, Italy.
[21]Also at CERN, 1211 Geneva 23, Switzerland.
[22]Supported by the US Department of Energy, grant DE-FG03-92ER40689.
[23]Now at DESY, Hamburg, Germany.
[24]Now at Lawrence Berkeley Laboratory, Berkeley, CA 94720, USA.
[25]Partially supported by Colciencias, Colombia.
[26]Also at Istituto di Matematica e Fisica, Università di Sassari, Sassari, Italy.
[27]Now at University of Athens, 157-71 Athens, Greece.

1 Introduction

The Standard Model of the electroweak interaction is extremely successful in explaining the wealth of precision measurements provided by the LEP experiments on the neutral current. Similarly, the most precise data on the Lorentz structure of the charged current, obtained through the study of μ decay [1, 2], is in excellent agreement with the Standard Model V-A expectation. Nevertheless, a global analysis of the μ decay parameters, the Michel parameters ρ, η, ξ, δ [3, 4], leaves room for non–Standard Model contributions to μ decay [5]. Not only is the larger mass of the τ–lepton strong motivation to search for deviations from V-A in its decay but the τ also offers the possibility to investigate lepton universality and, to determine the τ–neutrino helicity from its hadronic decays. Thus, the τ lepton is a unique probe in the study of the charged current interaction.

This paper describes an extension to leptonic τ decays of the correlation measurement, using the ALEPH detector at LEP, presented in [6]. The abundant production of τ–pairs on the Z resonance through the neutral current and the nearly perfect anti-correlation of the helicities of the τ^+ and τ^- allow the detailed investigation of the τ decay. From the analysis of the correlated spectra in the observables used in the polarisation analysis [7], production and decay parameters are simultaneously extracted. Assuming V and A type couplings in the neutral current, the only parameter to describe the production after integration over the production angle is the mean τ polarisation, p_τ. The decay parameters are the Michel parameters ρ_ℓ, η_ℓ, ξ_ℓ, $(\xi\delta)_\ell$ for leptons and the τ neutrino helicity $h(\nu_\tau) = \xi_h$ for hadrons.

2 Method

The leptonic decays $\tau^- \to \ell^- \bar{\nu}_\ell \nu_\tau$ can be described by the most general, four–fermion contact interaction. As the charged weak current is seen to be dominated by couplings to left–handed fermions the matrix element is written in the helicity projection form [8, 9]

$$\mathcal{M} = \frac{4G_\ell}{\sqrt{2}} \sum_{\substack{\gamma=S,V,T \\ i,j=L,R}} g^\gamma_{ij} \langle \bar{\ell}_i | \Gamma^\gamma | (\nu_\ell)_m \rangle \langle (\bar{\nu}_\tau)_n | \Gamma_\gamma | \tau_j \rangle \tag{1}$$

where G_ℓ is a constant equivalent to the Fermi constant in $\mu^- \to e^- \bar{\nu}_e \nu_\mu$. This matrix element contains ten complex coupling constants, g^γ_{ij} where the type of interaction – $\Gamma^S = 1$ for scalar, $\Gamma^V = \gamma^\mu$ for vector, $\Gamma^T = \frac{1}{\sqrt{2}}\sigma^{\mu\nu}$ for tensor – is labelled by γ and the chiral projections of the leptons – left, right – by i and j. The neutrino helicities n, m are uniquely determined for given γ and i, j. In the Standard Model V-A interaction the only non–zero coupling constant is $g^V_{LL} = 1$. The amplitude (1) leads to the decay distribution [8]

$$\begin{aligned} \frac{1}{\Gamma}\frac{d\Gamma}{dz} &= F_\ell(z) - p_\tau \cdot G_\ell(z) \\ &= f_c(z) + \rho_\ell \cdot f_\rho(z) + \eta_\ell \cdot f_\eta(z) - p_\tau \cdot \Big(\xi_\ell \cdot g_\xi(z) + (\xi\delta)_\ell \cdot g_{\xi\delta}(z) \Big) \end{aligned} \tag{2}$$

where the Michel parameters ρ_ℓ, η_ℓ, $(\xi\delta)_\ell$, ξ_ℓ are bilinear combinations of the g^γ_{ij}'s [8], p_τ is the τ polarisation and $z = \frac{E_\ell}{E_\tau}$ the normalised laboratory lepton energy. Excluding radiative corrections and non–multiplicative mass terms, the functions f and g are simple polynomials as illustrated for $\tau \to \mu \bar{\nu}_\mu \nu_\tau$ in Figure 1. Standard Model predictions for ρ_ℓ, η_ℓ, $(\xi\delta)_\ell$, ξ_ℓ are respectively $\frac{3}{4}, 0, \frac{3}{4}, 1$ – independent of the final state lepton.

The parameters ρ_ℓ, ξ_ℓ and $(\xi\delta)_\ell$ can be used to place limits on several of the complex coupling constants g^γ_{ij}. An interesting combination is

$$P^\tau_R = \frac{1}{2}\left(1 + \tfrac{1}{3}\xi_\ell - \tfrac{16}{9}(\xi\delta)_\ell\right) = \quad \frac{1}{4}|g^S_{RR}|^2 + \frac{1}{4}|g^S_{LR}|^2 + |g^V_{RR}|^2 + |g^V_{LR}|^2 + 3|g^T_{LR}|^2 \tag{3}$$

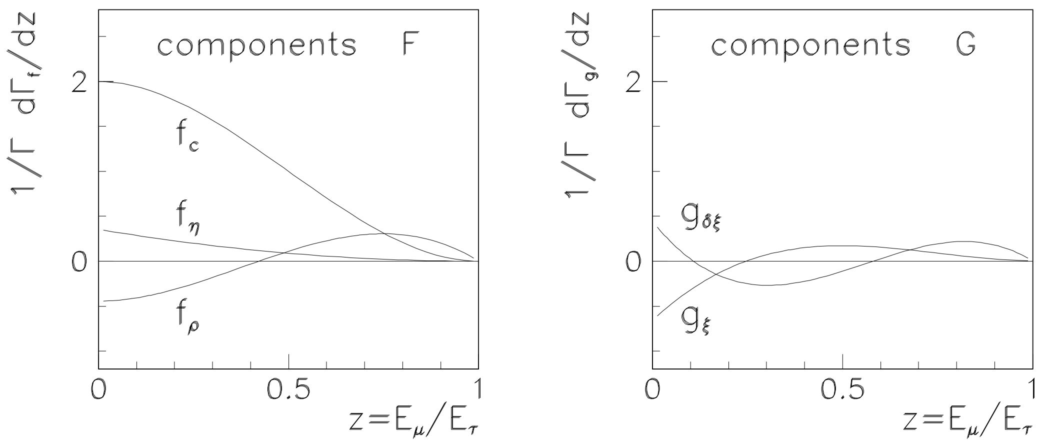

Figure 1: Spectral components of the F and G functions without radiative corrections and non-multiplicative mass terms for $\tau \to \mu \bar{\nu}_\mu \nu_\tau$.

which measures the total contribution of right-handed τ-couplings to the decay [9].

In the search for small deviations from a dominant V-A interaction, the quadratic dependence of ρ_ℓ, ξ_ℓ and $(\delta\xi)_\ell$ on the non–standard couplings is a drawback. The η_ℓ parameter receives a linear contribution from the interference of the expectedly dominant Standard Model coupling, g^V_{LL}, with a Higgs–like coupling, g^S_{RR} [9].

For $p_\tau = 0$, i.e. when τ pairs are produced in the decay of a virtual photon, the energy distribution of the lepton in the laboratory only allows the measurement of the two parameters ρ_ℓ and η_ℓ. The function f_η contains a multiplicative factor proportional to $\frac{m_\ell}{m_\tau}$ so that the electron decay channel has no sensitivity to η_e. In addition, the highest sensitivity to η_μ is in the low z region which has the lowest detection efficiency.

For $p_\tau \neq 0$ the energy distribution is also sensitive to ξ_ℓ and $(\delta\xi)_\ell$ but it is impossible to separately determine all five parameters including p_τ. Even with p_τ known, it is not possible to deduce ρ_ℓ, η_ℓ, ξ_ℓ and $(\delta\xi)_\ell$ from the energy distribution alone.

For V and A type couplings in the production amplitude, the helicities of the τ^+ and τ^- are opposite. From an analysis of the correlated decay spectra all the parameters can be extracted up to a sign ambiguity [9, 10] which can be resolved using input from other experiments.

For the hadronic modes the decay distribution can also be written in the generic form (2) [6, 9, 10]:

$$\begin{aligned} \frac{1}{\Gamma}\frac{d\Gamma}{dz} &= F_h(z) - p_\tau \cdot G_h(z) \\ &= f(z) - p_\tau \cdot \xi_h \cdot g(z), \end{aligned} \tag{4}$$

where f and g are purely kinematic functions. For the decay $\tau \to \pi \nu_\tau$ the polarisation sensitive variable is $z = \frac{E_\pi}{E_\tau}$, for the decays $\tau \to a_1 \nu_\tau$ and $\tau \to \rho \nu_\tau$, z is identical to the ω variable introduced in [7, 11], and for all other decays $z = \frac{E}{E_\tau}$, with E the energy of the decay product(s). For the simple case $\tau^- \to \pi^- \nu_\tau$ it is straightforward to show that $\xi_h = \xi_\pi$ corresponds to the τ neutrino helicity, $h(\nu_\tau)$.

The correlated spectra for modes i, j can now be written as

$$\frac{1}{\Gamma}\frac{d^2\Gamma}{dz_i dz_j} = F_i(z_i)F_j(z_j) + G_i(z_i)G_j(z_j) - p_\tau \cdot [G_i(z_i)F_j(z_j) + G_j(z_j)F_i(z_i)] \tag{5}$$

where the dependence on the parameters $\rho_\ell, \eta_\ell, \xi_\ell, (\delta\xi)_\ell$ for the leptons and on ξ_h for the hadrons is implied. The sign of p_τ is determined by the polarisation asymmetry measurement [7] and the SLD measurement of A_{LR} [12]. Alternatively, the sign of ξ_{a_1} is known from the parity violation measurement at ARGUS [13]. Thus, all sign ambiguities are resolved.

3 Data Analysis

The analysis uses $40.3\,pb^{-1}$ of data, about 5×10^4 produced $\tau^+\tau^-$ pairs, recorded with the ALEPH detector in the years 1990 to 1992. A detailed description of the detector can be found in [14]. The event preselection, the charged particle identification based on a neural network, and the decay mode classification are detailed in [7]. Modes which are not explicitly reconstructed as e, μ, π, ρ, $a_1 \to 3\pi^\pm$ are classified as X. Kaons are not distinguished from pions. The X candidate must have one or three tracks. The sum of track and photon energies is used as an estimator of its energy.

Only τ pair candidate events in which at least one of the τ decays is classified as e, μ, π, ρ, a_1 are retained. The z variables are computed for each of the two candidate decays in the event according to the prescription outlined in the previous section. The events are divided into exclusive groups consisting of all candidate lepton-lepton, lepton-hadron, hadron-hadron, lepton-X, and hadron-X. The ee group is excluded to avoid Bhabha events. No charge separation is made.

The event preselection accepts all low multiplicity events. Bhabha, μ-pair and two-photon events are, unlike [7], removed through cuts on the single particle energy in the same side hemisphere and on the event total energy. These cuts define clean borders in the kinematic distributions which are easily included in the fitting procedure.

The background fractions and efficiencies are extracted from Monte Carlo generated events. A background event is defined as a $\tau^+\tau^-$–event in which one or both τ hemispheres are wrongly classified, or as a non–τ event which is falsely identified as a τ event. The number of reconstructed events, the average acceptance, and the average expected background fraction are summarised in Table 1. The background is dominated by misidentified τ decays.

Each year of data gives a set of nineteen two-dimensional arrays with 15×15 equally sized bins. Due to the energy scans in 1990-91 and slight year to year variations in efficiency and background the data sets are treated independently.

4 Parameter Extraction

The two-dimensional spectra of the expected number of events, E, are fit to the observed distributions N using the method described in [6]. The negative logarithm of the likelihood function

$$\mathcal{L} \;=\; \prod_{i,j,ab} \frac{e^{-E(\mathcal{P};i,j,ab)}E(\mathcal{P};i,j,ab)^{N(i,j,ab)}}{N(i,j,ab)!}$$

is minimised with respect to the parameter set $\mathcal{P} = \{p_\tau, \rho_\ell, \eta_\ell, (\delta\xi)_\ell, \xi_\ell, \xi_h\}$. The indices i, j run over all the bins in the fit range except for the symmetric groups, for which the spectra are folded across the diagonal, so that $i \geq j$. $N(i,j,ab)$ is the number of observed events in the kinematic bin (i,j) for group ab.

The expected spectra are the sum of the predicted signal events, S, and the τ and non-τ background, B:

$$E(\mathcal{P};i,j,ab) \;=\; S(\mathcal{P};i,j,ab) + B(i,j,ab).$$

Table 1: Number of reconstructed events, the average efficiency $\langle\varepsilon\rangle$, and the expected background from τ and non-τ sources for each event group (* 1992 data only).

group	events reconstructed	$\langle\varepsilon\rangle$ [%]	estimated background [%] τ	non-τ
$e\mu$	2407	70.4 ± 0.3	3.2 ± 0.2	0.6 ± 0.1
$e\pi$	1208	45.6 ± 0.5	8.7 ± 0.4	0.7 ± 0.1
$e\rho$	1894	37.7 ± 0.4	9.2 ± 0.4	0.3 ± 0.1
ea_1	775	41.5 ± 0.6	10.1 ± 0.5	0.5 ± 0.1
eX	3179	52.6 ± 0.3	2.1 ± 0.1	0.6 ± 0.1
$\mu\mu$	1298	63.5 ± 0.4	3.1 ± 0.2	2.0 ± 0.3
$\mu\pi$	1387	55.5 ± 0.4	7.9 ± 0.3	0.5 ± 0.1
$\mu\rho$	2249	45.7 ± 0.4	7.9 ± 0.3	0.4 ± 0.1
μa_1	918	50.3 ± 0.6	9.4 ± 0.5	0.1 ± 0.1
μX	4482	64.0 ± 0.3	1.6 ± 0.1	0.1 ± 0.3
$\pi\pi$	399	45.5 ± 0.8	12.2 ± 0.8	1.1 ± 0.4
$\pi\rho$	1269	39.4 ± 0.5	12.4 ± 0.4	1.5 ± 0.2
πa_1	527	42.2 ± 0.7	14.9 ± 0.8	0.2 ± 0.1
πX	2769	58.9 ± 0.3	7.1 ± 0.2	0.8 ± 0.3
$\rho\rho$	987	29.9 ± 0.5	12.4 ± 0.5	2.4 ± 0.4
ρa_1	852	32.8 ± 0.5	13.6 ± 0.6	0.6 ± 0.1
ρX	4368	42.2 ± 0.3	7.3 ± 0.2	0.1 ± 0.1
$(a_1 a_1)^*$	119	36.0 ± 1.5	15.4 ± 1.6	0.1 ± 0.2
$(a_1 X)^*$	1142	47.7 ± 0.5	8.7 ± 0.4	0.1 ± 0.1

Small changes in the background distributions due to the difference between the Monte Carlo Standard Model polarisation and the fitted value are included in the systematic uncertainties (see below).

On including QED radiative corrections the theoretical spectra from (2) and (4) are transformed to $\hat{T}$. Following the suggestions in [15] the transformation proceeds in two steps:

- the functions F and G, obtained by an analytic method for e, μ, π and by simulation for the others, are modified to include final state radiation.
- the spectra are convoluted with a radiator function which describes the τ energy loss due to initial state radiation.

To obtain the signal distribution, the spectra $\hat{T}$ are subsequently folded with resolution and efficiency matrices, $\mathcal{R}$ and ε, determined from simulation. The matrix $\mathcal{R}$ describes the transition from the calculated spectrum to the measured one and accounts for detector resolution and bremsstrahlung in the detector material. The signal distributions are

$$S(\mathcal{P}; i, j, ab) \quad = \quad \varepsilon(i, j, ab) \sum_{i', j'} \hat{T}(\mathcal{P}; i', j', ab) \mathcal{R}(i, i', j, j', ab)$$

For the groups with X candidates the signal distributions contain additional terms which describe the feedthrough from unidentified e, μ, π, ρ, a_1. The absolute contribution of these feedthrough channels to the signal distribution is about 53%: 1% e, 3% μ, 7% π, 32% ρ, and 10% $a_1 \rightarrow 3\pi^{\pm}$, with slight variations between data sets. The relative composition is defined by

Table 2: Fit results with and without the universality assumption.

with universality		without universality	
p_τ	-0.132 $\pm$ 0.015	p_τ	-0.132 $\pm$ 0.015
ρ_ℓ	0.751 $\pm$ 0.039	ρ_e	0.793 $\pm$ 0.050
		ρ_μ	0.693 $\pm$ 0.057
$(\xi\delta)_\ell$	0.88 $\pm$ 0.11	$(\xi\delta)_e$	1.11 $\pm$ 0.17
		$(\xi\delta)_\mu$	0.71 $\pm$ 0.14
ξ_ℓ	1.18 $\pm$ 0.15	ξ_e	1.03 $\pm$ 0.23
		ξ_μ	1.23 $\pm$ 0.22
η_ℓ	-0.04 $\pm$ 0.15	η_μ	-0.24 $\pm$ 0.23
		ξ_π	-0.987 $\pm$ 0.057
ξ_h	-1.006 $\pm$ 0.032	ξ_ρ	-1.045 $\pm$ 0.058
		ξ_{a_1}	-0.939 $\pm$ 0.116

the ratio of branching ratios, $f_b = \frac{B_b}{B_X}$, and the inefficiency matrices, $\bar{\varepsilon}$.

$$\begin{aligned} S(\mathcal{P}; i, j, aX) &= \varepsilon(i,j,aX) \sum_{i',j'} \hat{T}(\mathcal{P}; i', j', aX)\mathcal{R}(i, i', j, j', aX) \\ &\quad + \sum_{b,i',j'} f_b \hat{T}_x(\mathcal{P}; i', j', ab)\mathcal{R}_x(i, i', j, j', ab)\bar{\varepsilon}(i,j,ab) \end{aligned}$$

The subscript x indicates that the polarisation sensitive variable for the unidentified modes $b = \rho, a_1$ is $\frac{E}{E_\tau}$ instead of ω.

The expected distribution of events in a group is normalised to the number of observed events in this group

$$\sum_{i,j} E(\mathcal{P}; i, j, ab) = N(ab).$$

The results of the fit are given in Table 2. The values in the left column are obtained with the assumption of e–μ universality in the charged current. The corresponding values without universality are given in the right column. Both fits have a $\chi^2/Dof = 0.993$. The correlation coefficients for the fit with universality are reproduced in Table 3. Excluding the groups with X results in similar values for the parameters but 10-20% larger statistical errors.

On comparing values or errors in Table 2 it is important to recall that η_ℓ is entirely determined from the μ spectrum because of the $\frac{m_\ell}{m_\tau}$ suppression and, that η_ℓ and ρ_ℓ are highly correlated. Thus, the different errors on η_ℓ and η_μ in Table 2 are purely due to the different correlations between ρ_μ–η_μ and ρ_ℓ–η_ℓ. The latter correlations are smaller because of the additional and independent information on ρ_ℓ from the e–spectrum. Similarly, the difference between ρ_μ and ρ_e is an artifact of the large negative value for η_μ. Setting $\eta_\mu = 0$ shifts ρ_μ up by 0.05 to 0.744.

Table 3: Correlation coefficients for fit with universality.

	ρ_ℓ	$(\xi\delta)_\ell$	η_ℓ	ξ_ℓ	ξ_h
p_τ	-0.43	-0.08	0.01	0.00	0.39
ρ_ℓ	1	0.03	0.42	0.05	0.56
$(\xi\delta)_\ell$		1	0.16	0.03	0.33
η_ℓ			1	0.36	0.67
ξ_ℓ				1	0.05

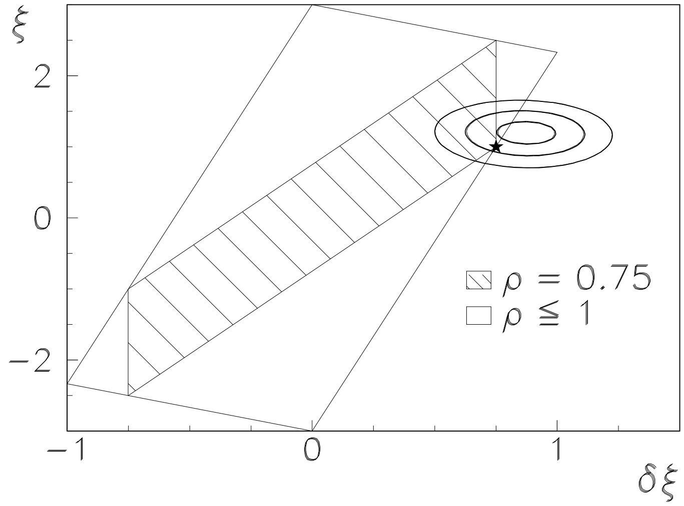

Figure 2: Contour levels in 1σ steps of $\ln\mathcal{L}$, corresponding to 39%, 63%, and 78% probability, in the $(\delta\xi)_\ell$ - ξ_ℓ plane. The open trapezoid encloses the physically allowed region. The hatched area delimits the allowed region for $\rho = 0.75$, and the V-A expectation is marked by $\star$.

Figure 2 shows the 1-3σ contour levels of $\ln\mathcal{L}$ in the $(\delta\xi)_\ell$-ξ_ℓ plane. Thus, it is expected that the measurements of $(\delta\xi)_\ell$ and ξ_ℓ will limit the allowed ranges of the coupling constants, g^γ_{ij}.

The distributions for the final state particles, obtained from projections of the corresponding two–dimensional spectra, in Figure 3 compare the observed and the best-fit spectra in the polarisation sensitive variable.

5 Systematic Uncertainties

The major sources of systematic errors are uncertainties in acceptance, resolution, and background rates. These errors, their origins and their effect on the uncorrelated spectra and the polarisation are detailed in [7] and their influence on the measurements have been investigated. In addition, consideration is given to errors which may only become apparent in the correlation analysis or are intrinsic to the method.

The effect of an incorrect modelling of the background levels is determined by rescaling the whole background and/or the separate contributions from τ and non-τ sources by $\pm 20\%$. The influence of the shape of the τ background is studied by varying the ξ_h value and the overall polarisation of the background by $\pm 1\sigma$ of the fitted values. No change with respect to ξ_h is observed.

Detailed studies show that the simulation correctly models the energy response of the detector [7]. Nevertheless, a slight energy dependent difference between the efficiencies obtained from Monte Carlo and data cannot be excluded. To reflect this uncertainty the efficiencies are modified by polynomial functions obtained from the ratio of data to simulated efficiencies.

The uncertainty in the theoretical model describing $\tau \to a_1\nu_\tau$ and its influence on ξ_{a_1} is computed in the same fashion as the uncertainty on the polarisation from the a_1 channel [7]. The extent to which the crossover ratios influence the fit is investigated by varying the branching fractions within 1σ subject to the constraint that they sum to unity.

Finally, the acceptance and resolution matrices contain intrinsic uncertainties due to the finite Monte Carlo set used in their determination. The resulting statistical fluctuations in these

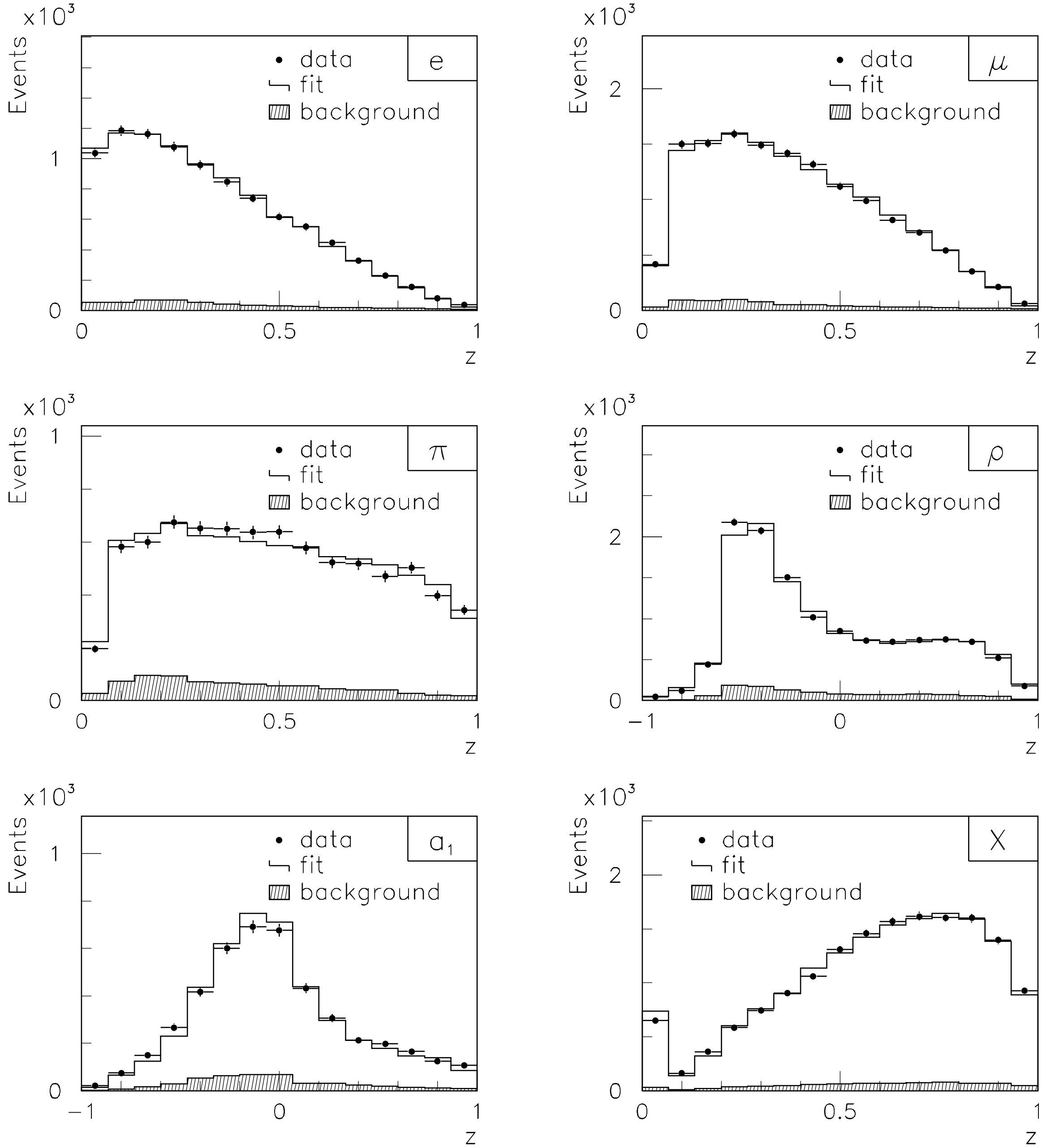

Figure 3: Particle spectra in the polarisation sensitive variable for the various final states.

matrices are not directly incorporated into the fitting procedure and are thus included as an additional systematic uncertainty.

A summary of the systematic uncertainties in the parameters are given in Table 4 and Table 5.

Table 4: Systematic uncertainties for parameters with universality assumption.

	p_τ	ρ_ℓ	η_ℓ	$(\delta\xi)_\ell$	ξ_ℓ	ξ_h
background	0.006	0.012	0.09	0.01	0.02	0.007
efficiency	0.007	0.012	0.05	0.06	0.03	0.012
crossover	0.003	0.003	0.02	0.01	-	0.005
theory a_1	0.002	0.001	-	-	-	0.003
MC statistics	0.005	0.013	0.05	0.04	0.05	0.011

Table 5: Systematic uncertainties for parameters without universality assumption.

	ρ_e	ρ_μ	η_μ	$(\delta\xi)_e$	$(\delta\xi)_\mu$	ξ_e	ξ_μ	ξ_π	ξ_ρ	ξ_{a_1}
background	0.014	0.018	0.10	0.03	0.03	0.02	0.06	0.006	0.011	0.005
efficiency	0.010	0.011	0.12	0.02	0.01	0.03	0.04	0.019	0.021	0.019
crossover	0.004	0.005	0.01	0.01	0.01	0.01	0.01	0.003	0.011	0.005
theory a_1	-	-	-	-	-	-	-	0.002	0.002	0.050
MC statistics	0.017	0.019	0.08	0.06	0.05	0.08	0.07	0.019	0.019	0.039

6 Results and Conclusions

Within the framework of V and A type couplings in the production of τ pairs at the Z resonance the Michel parameters in the decays $\tau \to \ell \bar{\nu}_\ell \nu_\tau$ have been measured. The results from this analyis

$$\begin{array}{rcllll} \rho_\ell & = & 0.751 & \pm & 0.039 & \pm & 0.022 \\ \eta_\ell & = & -0.04 & \pm & 0.15 & \pm & 0.11 \\ \xi_\ell & = & 1.18 & \pm & 0.15 & \pm & 0.06 \\ (\delta\xi)_\ell & = & 0.88 & \pm & 0.11 & \pm & 0.07 \\ \langle h(\nu_\tau) \rangle = \xi_h & = & -1.006 & \pm & 0.032 & \pm & 0.019 \end{array}$$

are to be compared with the Standard Model values of $\frac{3}{4}, 0, 1, \frac{3}{4}, -1$, respectively. In addition, the τ polarisation has been determined as $p_\tau = -0.132 \pm 0.015 \pm 0.011$. This value is in very good agreement with the preliminary value of $-0.134 \pm 0.12 \pm 0.008$ obtained with the same statistics by the standard τ polarisation analysis at ALEPH with the V-A assumption in the charged current [16]. Neither of these values contains corrections for γZ interference or electroweak radiative effects.

Taking into account all correlations and including the systematic uncertainties, one can determine an upper bound on the contribution of right–handed τ–couplings to the decay. In the Bayesian approach for obtaining one–sided limits [17], this leads to $P_R^\tau \leq 0.24$ at 90% confidence level.

If the charged current interaction does not obey the universality condition, then the following measurements hold:

$$\begin{array}{rcllllll} \rho_e & = & 0.793 & \pm & 0.050 & \pm & 0.025 \\ (\delta\xi)_e & = & 1.11 & \pm & 0.17 & \pm & 0.07 \\ \xi_e & = & 1.03 & \pm & 0.23 & \pm & 0.09 \\ \xi_\pi & = & -0.987 & \pm & 0.057 & \pm & 0.027 \\ \xi_{a_1} & = & -0.937 & \pm & 0.116 & \pm & 0.064\,. \end{array}$$

$$\begin{array}{rcllllll} \rho_\mu & = & 0.693 & \pm & 0.057 & \pm & 0.028 \\ \eta_\mu & = & -0.24 & \pm & 0.23 & \pm & 0.18 \\ (\delta\xi)_\mu & = & 0.71 & \pm & 0.14 & \pm & 0.06 \\ \xi_\mu & = & 1.23 & \pm & 0.22 & \pm & 0.10 \\ \xi_\rho & = & -1.045 & \pm & 0.058 & \pm & 0.032 \end{array}$$

The ξ_h measurements presented here supersede those previously obtained with lower statistics [6].

For the first time the Michel parameter $(\delta\xi)_\ell$ has been measured in τ decays. The measurements of the other parameters, $\rho_\ell, \eta_\ell, \xi_\ell, \xi_h$ are in good agreement with other experiments [13, 17, 18] or inferred values [19]. None of these measurements shows disagreement with Standard Model expectation at the current level of precision.

Acknowledgements

It is a pleasure to thank the technical personnel of the collaborating institutions for their support in constructing and maintaining the ALEPH experiment. Those of the collaboration not from member states thank CERN for its hospitality.

References

[1] H. Burkhard et al., Phys. Lett. B 160 (1985) 343.

[2] B. Balke et al., Phys. Rev. D 37 (1988) 587.

[3] L. Michel, Proc. Phys. Soc. A 63 (1950) 514; C. Bouchiat and L. Michel, Phys. Rev. 106 (1957) 170.

[4] T. Kinoshita and A. Sirlin, Phys. Rev. 108 (1957) 844.

[5] W. Fetscher, H.-J. Gerber, and K.F. Johnson, Phys. Lett. B 173 (1986) 102.

[6] ALEPH Collab., D. Buskulic et al., Phys. Lett B 321 (1994) 168.

[7] ALEPH Collab., D. Buskulic et al., Z. Phys. C 59 (1993) 369.

[8] F. Scheck, Phys. Rep. 44 (1978) 187; Leptons, Hadrons and Nuclei (North-Holland, Amsterdam, 1983).

[9] W. Fetscher, Phys. Rev. D 42 (1990) 1544.

[10] C. Nelson, Phys. Rev. D 40 (1989) 123; Erratum: Phys. Rev. D 41 (1990) 2327.

[11] M. Davier, L. Duflot, F. Le Diberder, and. A. Rougé, Phys. Lett. B 306 (1993) 411.

[12] SLD Collab., K. Abe et al., Phys. Rev. Lett. 70 (1993) 2515.

[13] ARGUS Collab., H. Albrecht et al., Z. Phys. C 58 (1993) 61.

[14] ALEPH Collab., D. Decamp et al., Nucl. Instr. Meth. A 294 (1990) 211; CERN-PPE 94–170, (1994).

[15] S. Jadach and Z. Was, Z Physics at LEP I, CERN 89-08, eds. G. Altarelli, et al. .

[16] ALEPH Collab., Contribution to the 27th International Conference on High Energy Physics, Glasgow, Scotland, July 1994.

[17] Particle Data Group, Phys. Rev. D 50 (1994).

[18] ARGUS Collab., H. Albrecht et al., Phys. Lett. B 316 (1993) 608; Phys. Lett. B 337 (1994) 383; DESY-94-100 (1994).

[19] A. Stahl, Phys. Lett. B 324 (1994) 121.